Available online at www.sciencedirect.com
ScienceDirect
Atmospheric Environment 42 (2008) 2630–2642
ATMOSPHERIC ENVIRONMENT
www.elsevier.com/locate/atmosenv

Light scattering and absorption properties of aerosol particles in the urban environment of Granada, Spain

H. Lyamani[a,b], F.J. Olmo[a,b], L. Alados-Arboledas[a,b,*]

[a]*Departamento de Física Aplicada, Facultad de Ciencias, Universidad de Granada, Fuentenueva s/n. 18071, Granada, Spain*
[b]*Centro Andaluz de Medio Ambiente (CEAMA), Junta de Andalucía-Universidad de Granada, Avda. del Mediterraneo s/n. 18071, Granada, Spain*

Received 7 December 2006; received in revised form 22 October 2007; accepted 26 October 2007

Abstract

Surface measurements of optical and physical aerosol properties were made at an urban site, Granada (Spain) (37.18°N, 3.58°W, 680 m a.s.l), during winter 2005–2006. Measurements included the aerosol scattering, σ_{sca}, and backscattering coefficients, σ_{bsca}, at three wavelengths (450, 550 and 700 nm) measured at low relative humidity (RH < 50%) by an integrating nephelometer, the absorption coefficient at 670 nm, σ_{abs}, measured with a multi-angle absorption photometer, and aerosol size distribution in the 0.5–20 μm aerodynamic diameter range registered by an aerodynamic aerosol sizer (APS-3321, TSI). The hourly average of σ_{sca} (550 nm) ranged from 2 to 424 M m^{-1} with an average value of 84 ± 62 M m^{-1} ($\pm$S.D.). The Angstrom exponent presented an average value of 1.8 ± 0.3, suggesting a large fraction of fine particles at the site, an observation confirmed by aerosol size distribution measurements. The hourly average of σ_{abs} (670 nm) ranged from 1.7 to 120.5 M m^{-1} with an average value of 28 ± 20 M m^{-1}. The results indicate that the aerosol absorption coefficient in Granada was relatively large. The largest σ_{sca} value was associated with air masses that passed over heavily polluted European areas and local stagnation conditions. High absorbing aerosol level was obtained during dust transport from North Africa probably due to the presence of hematite. Based on the measured scattering and absorption coefficients, a very low average value of the single scattering albedo of 0.66 ± 0.11 at 670 nm was calculated, suggesting that urban aerosols in this region contain a large fraction of absorbing material. A clear diurnal pattern was observed in scattering and absorption coefficients and particle concentrations with two local maxima occurring in early morning and late evening. This behavior can be explained in terms of local conditions that control the particle sources associated with traffic and upward mixing of the aerosol during the daytime development of a convective boundary layer. Significant reduction in absorption coefficient values has been found during weekends compared to working days, showing a strong impact of local sources on aerosol properties. In contrast to σ_{abs}, the aerosol scattering coefficient obtained during weekends was higher than those obtained on Mondays and Tuesdays. A possible explanation for the large values of σ_{sca} measured during the weekend could be secondary aerosol aging.

Keywords: Light scattering coefficient; Light absorption coefficient; Aerosol optical properties; Urban aerosol

*Corresponding author at: Departamento de Física Aplicada, Facultad de Ciencias, Universidad de Granada, Fuentenueva s/n. 18071, Granada, Spain. Tel.: +34 958 244024; fax: +34 958 243214.
E-mail address: alados@ugr.es (L. Alados-Arboledas).

1352-2310/$ - see front matter © 2007 Elsevier Ltd. All rights reserved.
doi:10.1016/j.atmosenv.2007.10.070

1. Introduction

Atmospheric aerosols have a significant impact on regional air pollution as well as on the radiation budget. Atmospheric aerosols directly affect the Earth's radiative budget by absorbing and scattering solar and thermal radiation (Haywood and Shine, 1997). Thus, in contrast to the greenhouse gases, which only cause warming, atmospheric aerosols, depending on their properties, can cause either cooling or warming of the atmosphere. Atmospheric aerosols also can indirectly affect the Earth's radiation balance and climate by changing the microphysical properties of clouds and their lifetimes (Kaufman et al., 2005), thereby modifying the precipitation regime. They play a major role in atmospheric chemistry and hence affect the concentrations of other minor atmospheric constituents like ozone. Furthermore, atmospheric aerosols have adverse effects on the human health, and a strong relationship between aerosol concentrations and human mortality and morbidity has been observed (Dockery and Pope, 1996). Atmospheric aerosols also have adverse effects on environmental quality including visibility (Waggoner et al., 1981; Horvath, 1995).

Many difficulties in assessing the climatic and environmental effects of atmospheric aerosols arise because of great spatial and temporal variability of their concentrations and physical and chemical properties. Hence, it is important to monitor aerosol physical, chemical and radiative properties at a wide range of sites around the globe, in order to build up a comprehensive picture of aerosols and their environmental impacts. To determine the influence of aerosols on climate, visibility and photochemistry, several key aerosol optical properties are required. These include the aerosol light extinction coefficient (the sum of the aerosol light scattering and absorption coefficients), aerosol single scattering albedo (the ratio of scattering to extinction coefficient), the aerosol upscatter fraction (the fraction of the incident solar radiation that is scattered upward to space), aerosol size distribution and the aerosol optical depth (e.g. Haywood and Shine, 1995; Waggoner et al., 1981). At this time, no studies have been reported on measurements of these important aerosol properties in the boundary layer in Spain. Columnar aerosol properties including aerosol optical depth over Granada (Spain) (37.18°N, 3.58°W, 680 m a.s.l) have been previously studied (Alados-Arboledas et al., 2003; Lyamani et al., 2005, 2006a, b). In order to complete the regular measurements of columnar atmospheric aerosol properties a surface aerosol monitoring station was installed in 2005 summer at Granada.

In this paper, surface measurements of aerosol optical properties at Granada, Spain, obtained during winter 2005–2006 are presented. Measurements included scattering and absorption coefficients as well as aerosol size distributions. Also shown are the meteorological parameters that influence these aerosol properties which include wind speed, ambient temperature and relative humidity (RH). Some aerosol episodes are investigated, through air mass origins, in order to identify the main source regions responsible for these special events. Diurnal and weekday variations of these parameters and the influence of meteorological conditions are also analyzed and explained.

2. Experimental site

The measurements presented in this study were made at an urban site Granada, from 1 December 2005 to 28 February 2006. Granada (37.18°N, 3.58°W, 680 m a.s.l) located in south-eastern Spain is a non-industrialized, medium-sized city with a population of 300 000, or 600 000 if the whole metropolitan area is considered. The city is situated in a natural basin surrounded by mountains with elevations between 1000 and 3500 m. The continental conditions prevailing at this site are responsible for large seasonal temperature differences, providing cool winters and hot summers. Most rainfall occurs during spring and wintertime. The study area is also at a short distance, about 200 km away from the African continent and approximately 50 km away from the western Mediterranean basin.

The site of study is located in the southern part of the city and is close to the highway that surrounds the city. The local aerosol sources are mainly the heavy traffic (mainly diesel vehicles) together with the re-suspension of material available on the ground. The old part of the city has rather narrow streets responsible of heavy traffic in some areas of the city, especially at rush hours. During winter, domestic heating (mainly diesel central heating) represents an additional important source of anthropogenic aerosols. Due to its location in the Mediterranean basin, it is influenced by two major aerosol source regions: Europe as a major source of anthropogenic pollutants and North Africa as principal source of natural dust. In fact, high levels

of aerosol have been reported when the study area was affected by air masses originated from Europe and North Africa (Lyamani et al., 2005, 2006a; Rodríguez et al., 2001). On other hand, forest fires represent an additional source of aerosol, but are not relevant for this winter study.

The bowl-like topography of Granada basin favors winter-time inversions and dominance of very weak wind speeds. This, in combination with pollutant emissions, mainly from traffic, can lead to a large accumulation of particles and thus high particles loads in the study area, which can cause environmental and human health problems. In fact, the haze over Granada basin often has a dark aspect, especially during morning, indicating the presence of soot particles as major pollutants in the basin.

3. Instruments and measurements

Surface observations were made from 1 December 2005 to 28 February 2006. Sample air for all measurements was obtained from the top of a stainless steel tube (20-cm diameter and 5-m length). The inlet is fitted with funnel covered by an insect screen to prevent rain drops and insects from getting into the sample line. The inlet was located about 15 m above the ground surface. The measurements were performed without aerosol size cut-off and no heating was applied to the sampled air. There is no bend in the tube that passes through the rooftop. Several stainless steel pipes located inside the stainless steel tube provided sampling air to the different instruments. Each one of the stainless pipes extracts the appropriate flow for each instrument. The excess flow is exhausted to the ambient by a high-capacity blower. The diameters of the pipes of the different instruments have been selected in order to optimize the efficiency of the system that has been designed to operate close to isokinetic conditions (Baron and Willeke, 2001). The design guarantees a laminar flow at the pipes of the different instruments, while sample flow in the main stack is turbulent due to the requirements for the total flow and isokinetic conditions.

The scattering (σ_{sca}) and backscattering coefficients (σ_{bsca}) were measured with an integrating nephelometer (TSI; model 3563) in three wavelengths 450, 550 and 700 nm. Calibration of the nephelometer was carried out by using CO_2 as high span gas and filtered air as low span gas. This instrument draws the ambient air through a temperature-controlled inlet at flow rate of $30\,l\,min^{-1}$. The averaging time was set to 5 min. The zero signal was measured once an hour.

Non-idealities due to non-lambertian and truncation errors were corrected using the method described by Anderson and Ogren (1998). To account for the particle-size dependence of the truncation error we used the correction equations based on the measured wavelength dependence of light scattering, as proposed by Anderson and Ogren (1998). Non-lambertian errors are most important for submicron particles whereas truncation errors are most important for micrometric particles (Anderson and Ogren, 1998). The non-lambertian error is the slightly non-cosine-weighted intensity distribution of light provided by the opal glass diffuser of the nephelometer. The truncation error is the geometrical blockage of scattered light for angle $<7^\circ$ and $>170^\circ$. For 5 min averaging time, the detection limits for total scattering coefficients are 0.44, 0.17, and $0.26\,M\,m^{-1}$ for 450, 550 and 700 nm, respectively (Anderson et al., 1996). For backscattering, the detection limits are 0.29, 0.11 and $0.21\,M\,m^{-1}$ for 450, 550 and 700 nm, respectively. Values below these detection limits are excluded.

Scattering by aerosols is strongly dependent on relative humidity, RH, due to the hygroscopic growth nature of most atmospheric aerosols (Horvath, 1996). The scattering coefficient shows a minimum variation below 50% relative humidity and a slow increasing behavior up to about 60% relative humidity (Anderson and Ogren, 1998; Xu et al., 2002). Above 80%, the scattering coefficient shows a sharp increase with relative humidity (Xu et al., 2002). Therefore, even if the particles are not chemically dry at RH < 50% they can be considered dry from a scattering point of view (Targino et al., 2005). During the study period, the relative humidity measured within the nephelometer chamber was in the range 8–50% and had mean values of $27 \pm 7\%$ which was lower than the ambient relative humidity of $58 \pm 14\%$. As a result, the light scattering measurements presented in this study can be considered as dry.

Light absorption was recorded with the recently introduced multi-angle absorption photometer (MAAP) (Thermo ESM Andersen Instruments, Erlangen, Germany). The MAAP results are based on simultaneous measurements of radiation transmitted through and reflected from a particle-loaded filter at two detection angles (Petzold and Schönlinner,

2004). The determination of the absorption coefficient of the filter-deposited aerosol uses a radiative transfer code and explicitly includes a treatment of scattering effects from the filter matrix and the light scattering aerosol component. The two-reflectivity measurements allow correction for multiple scattering processes involving the deposited particles and the filter matrix. A detailed description of the method is given by Petzold and Schönlinner (2004). The MAAP draws the ambient air at constant flow rate of $10001\,h^{-1}$ and operates at a wavelength of 670 nm. Mass absorption efficiency coefficient of $6.6\,m^2\,g^{-1}$ recommended by the manufacturer was used in the internal computations to convert the measured aerosol light absorption coefficient σ_{abs} to black carbon concentration [BC].

The study of Petzold et al. (2005) showed that the absorption coefficients measured by MAAP are in good agreement with those measured by photoacoustic spectrometry and the simultaneous measurement of aerosol extinction and aerosol scattering. Furthermore, the MAAP filter based method does not require calibration for the measurement of the aerosol absorption coefficient and does not need post-measurement data correction or parallel measurements of the aerosol light scattering coefficient (Petzold and Schönlinner, 2004; Petzold et al., 2005). The total method uncertainty for the aerosol light absorption coefficient inferred from MAAP measurement is around 12% (Petzold and Schönlinner, 2004; Petzold et al., 2005).

Particle size distribution and concentration measurements were conducted by an aerodynamic aerosol sizer (APS-3321; TSI). This instrument is an optical particle counter that measure particle diameter and aerosol concentration, in real time, in 52 nominal size bins in the diameter range 0.50–20 μm by determining the time-of-flight of individual particles in an accelerating flow field. The APS can measure concentrations up to 1000 particles cm^{-3} at 0.5 and 10 μm, with coincidence errors inferior to 5% and 10%, respectively. The minimum and maximum concentrations that can measure this instrument are 0.001 and 10 000 particles cm^{-3}, respectively. For solid particles, counting efficiencies range from 85% to 99% (Volcken and Peters, 2003). APS was operated at flow rate of $5\,l\,min^{-1}$ and with data averaging time of 5 min.

As in the case of the nephelometer, the air temperature inside the MAAP and the APS was slightly over the ambient temperature. The MAAP and APS, in contrast to the nephelometer, do not provide measurements of relative humidity of the sampled air. Taking into the account that the relative humidity inside the nephelometer during the study period was $<50\%$ and considering the temperature inside the nephelometer ($23\pm3\,^{\circ}C$), the MAAP ($26\pm2\,^{\circ}C$) and the APS ($32\pm2\,^{\circ}C$) we can conclude that inside the MAAP and APS the mean relative humidity was below 50%. Thus, all aerosol properties being measured can be considered intrinsic to the aerosol and not dependent on water content. In addition to these measurements, meteorological parameters (wind speed, ambient relative humidity and temperature) were measured at the sampling site.

Source regions causing special aerosol events can be detected by performing a back trajectory analysis. To characterize the transport pathways of air masses arriving at our study area and to detect the aerosol source regions responsible of some aerosol episodes in the study area, isentropic 5-day backward trajectories ending at 12 UTC at Granada for 500 m above ground level were calculated using the HYSPLIT model (Draxler and Rolph, 2003). The model version employed uses FLN data and includes vertical wind.

4. Results and discussion

4.1. Temporal variations in aerosol properties

Fig. 1 shows the variation of daily average values of light scattering, back scattering and absorption coefficients for the period from 1 December 2005 to 28 February 2006, and Table 1 presents a statistical summary of these data. The statistical data are calculated based on hourly averages. There was a significant day-to-day variability in all aerosol properties (Fig. 1). The daily average values of σ_{sca} (550 nm) ranged between 12 and $198\,M\,m^{-1}$ while σ_{abs} (670 nm) ranged from 4 to $46\,M\,m^{-1}$, which correspond to mean daily black carbon concentrations in the range 0.6–7.0 $\mu g\,m^{-3}$. The daily average values of backscattering coefficient at 550 nm varied from 1.7 to $21.1\,M\,m^{-1}$.

The largest scattering coefficient with σ_{sca} (550 nm) $= 198\,M\,m^{-1}$ was recorded on 22 January (Fig. 1a). This large aerosol light scattering level was associated with very weak wind ($0.7\pm0.4\,m\,s^{-1}$). In addition, a 5-day back trajectory analysis (Fig. 2) shows that the air mass that stagnated over

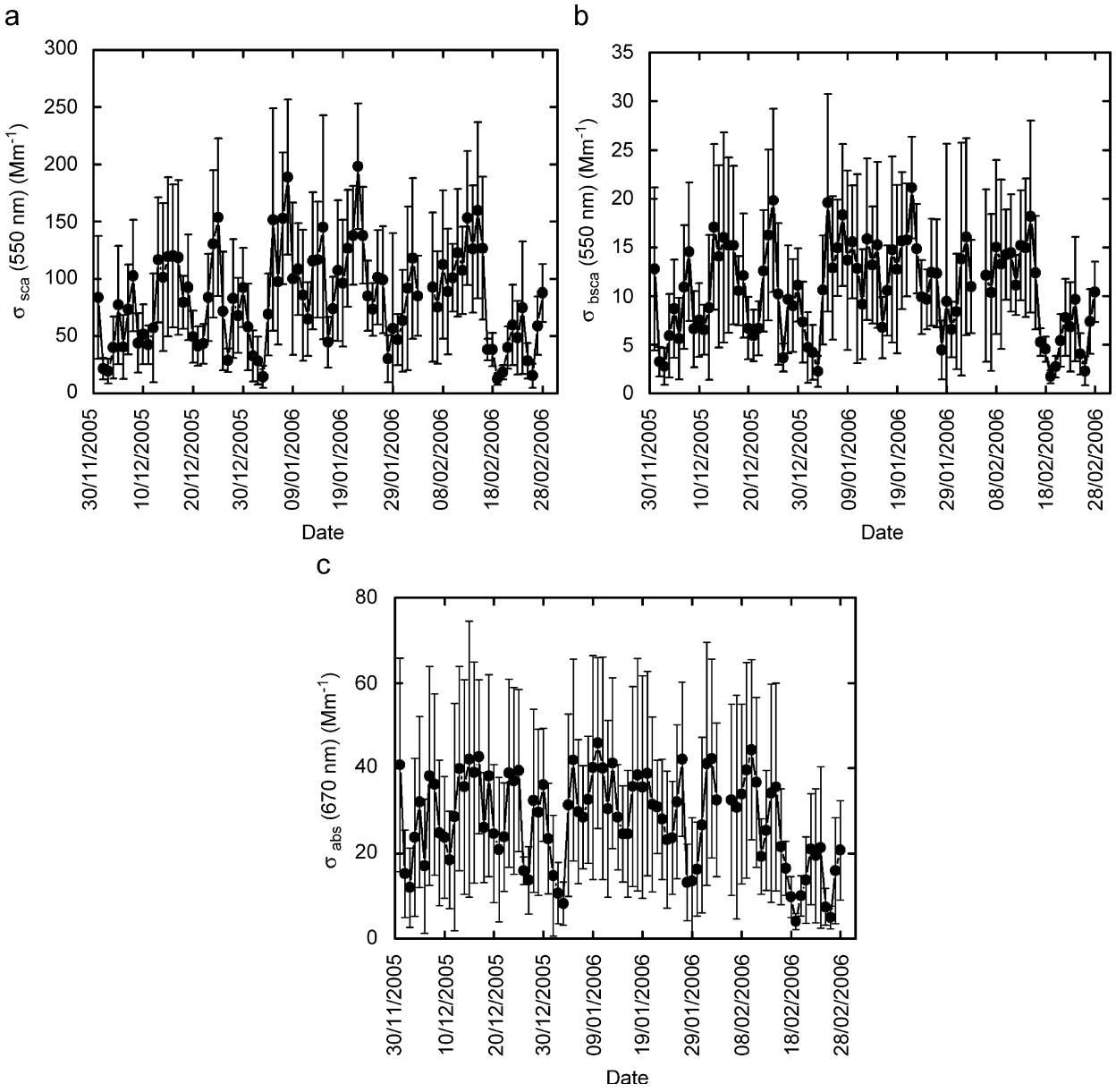

Fig. 1. Daily mean values and standard deviation of (a) aerosol scattering coefficient at 550 nm, (b) aerosol backscattering coefficient at 550 nm and (c) aerosol absorption coefficient at 670 nm for the period from 1 December 2005 to 28 February 2006. The vertical bars indicate standard deviations of data.

Granada at 500 m on 22 January had passed over polluted areas in Central Europe. Air masses originating in Europe are generally associated with high anthropogenic aerosol levels (Lyamani et al., 2006a). Thus, the European air mass contribution to the aerosol loading in the study area can explain the large scattering level reached on 22 January.

The largest absorption coefficient and hence the highest light absorbing aerosol concentration recorded on 10 January was linked to weak winds ($0.9 \pm 0.5\,m\,s^{-1}$) and dust transport from North Africa (Fig. 2). On this day, the air masses reaching the study area at 500, 1000 and 1500 m (above ground level) originated from North Africa. A possible explanation of the high absorption coefficient during this dust event is the presence of hematite. It is well known that hematite and black carbon are the main atmospheric aerosol components that

Table 1
Summary of aerosol properties (mean, standard deviation, maximum value, minimum value) measured in Granada, Spain, from 1 December 2005 to 28 February 2006

	Mean ± S.D.	Minimum–maximum	Percentile 25	Percentile 95
σ_{sca} (550 nm) (M m^{-1})	84 ± 62	2–424	38	206
σ_{bsca} (550 nm) M m^{-1})	11 ± 8	0.4–78.6	5.2	27.0
σ_{abs} (670 nm) M m^{-1})	28 ± 20	1.7–120.5	12.0	70.0
[BC] concentration (μg m^{-3})	4 ± 3	0.26–18.26	1.8	11.0
α	1.8 ± 0.3	0.3–2.3	1.6	2.0
ω_{0A} (670 nm)	0.66 ± 0.11	0.30–0.92	0.60	0.85
β_{sca} (550 nm)	0.13 ± 0.02	0.08–0.21	0.12	0.16

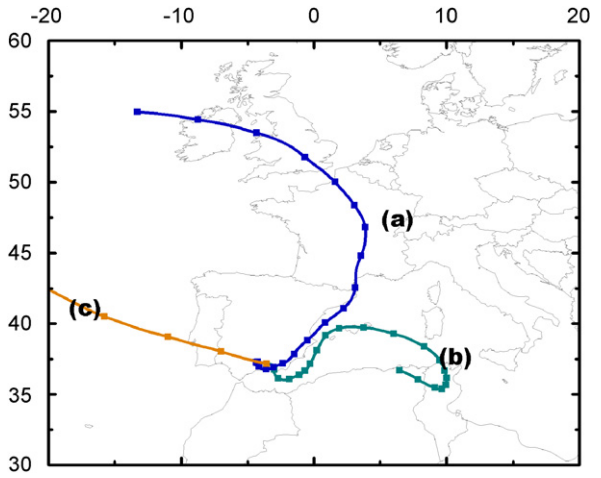

Fig. 2. Back trajectories ending at Granada at 12 UTC for altitude 500 m above ground level for (a) 22 January 2006, (b) 10 January 2006 and (c) 19 February 2006.

absorb radiation (Horvath, 1998; Bobren and Huffman, 1983).

The lowest σ_{sca} and σ_{abs} values were recorded on the same day on 19 February and were associated with a rain event and relatively high wind speeds of 3 ± 2 m s^{-1}. This is not a surprising result since precipitation scavenging is one of the most important atmospheric removal mechanisms. In addition, 5-day back trajectory analysis (Fig. 2) shows that air masses reaching Granada at 500 m on 19 February originated from the Atlantic Ocean. Aerosol scattering coefficient values as low as 5 M m^{-1} for marine air were measured in the Netherlands by ten Brink et al. (1996).

It is interesting to compare the measurements obtained here with results obtained in other urban sites. For instance, the aerosol absorption coefficient values obtained in Granada are in the range of σ_{abs} given by D'Almeida et al. (1991) for urban areas, 11.5–51.5 M m^{-1}. The mean aerosol absorption coefficient 28 ± 20 M m^{-1} obtained in this study at 670 nm is larger than the mean value of 16 ± 12 M m^{-1} obtained for this coefficient at 550 nm in the relatively polluted city of Atlanta, GA in the United States during August 1999 (Carrico et al., 2003). The mean black carbon concentration 4 ± 3 μg m^{-3} measured in Granada is much higher than [BC] = 0.9 μg m^{-3} obtained in the urban costal site, Toulon, France, during October–January 2005 (Saha and Despiau, 2006) and is slightly lower than the mean values of 5.21 and 6.58 μg m^{-3} obtained during winter 1998–1999 in Uji (Japan) and Vienna (Austria) by Hitzenberger and Tohno (2001). Furthermore, black carbon concentration obtained in Granada is in the range values of [BC] (3.00–4.25 μg m^{-3}) obtained during March 1997 in the relatively polluted urban area of Mexico City by Eidels-Dubovoi (2002).

As we can see, the aerosol absorption coefficients (and hence black carbon concentration) in Granada were in the range typical of relatively polluted areas. This result is somewhat surprising given that Granada is medium size and non-industrialized city. During winter time, the mean sources of pollutants in Granada are traffic, especially diesel vehicles, and domestic heating. The large absorption coefficient and black carbon concentration values obtained at Granada, comparable to the values reported for relatively polluted cities in the world (e.g. Atlanta and Mexico City), could be explained by the bowl-like topography of Granada and the very low wind speeds occurring during winter. Being surrounded by high mountains all around Granada and dominated by week wind speeds, the horizontal dispersion of the emitted pollutants out of the study area is limited, producing a large accumulation of all type of pollutants and leading to high aerosol loads over the study area. In fact, the haze is clearly visible and a dark layer is often viewed over the city.

Thus, it seems that aerosol concentration depends strongly on meteorological and topographical conditions. In this sense, Park et al. (2002) found that the difference between ambient BC levels (and hence absorption coefficient) in two cities in Korea was not proportional to the population ratio or diesel traffic ratio, and that the particulate matter or BC concentration is strongly influenced by varying traffic and meteorological conditions at the site.

The mean aerosol scattering coefficient at 550 nm $80 \pm 60\,\mathrm{M\,m^{-1}}$ obtained in Granada is within the range mean values of σ_{sca} (550 nm) (30–210 $\mathrm{M\,m^{-1}}$) reported for urban areas in the United States (Waggoner et al., 1981). However, the mean value of σ_{sca} (550 nm) obtained in this study is lower than the mean value of $120 \pm 50\,\mathrm{M\,m^{-1}}$ measured in Atlanta (relatively polluted city in the US) during August 1999 (Carrico et al., 2003). Nevertheless, the σ_{sca} values observed at Granada are relatively higher than those reported for the eastern Mediterranean region. A mean scattering coefficient of $65 \pm 40\,\mathrm{M\,m^{-1}}$ mainly resulting from continental pollution was observed in northern Greece by Gerasopoulos et al. (2003). Andreae et al. (2002) reported a mean scattering coefficient of $90 \pm 50\,\mathrm{M\,m^{-1}}$ in Israel as result of continental pollution and dust events. Also, the aerosol scattering values reported here are larger than those obtained in an urban area in East Baltimore (2–95 $\mathrm{M\,m^{-1}}$ with mean value of $32 \pm 19\,\mathrm{M\,m^{-1}}$, excluding forest fire event) by Adam et al. (2004). The mean value of backscattering coefficient at 550 of $6 \pm 4\,\mathrm{M\,m^{-1}}$, mainly resulting from continental pollution, reported for the region of Ouranoupolis, northern Greece, by Gerasopoulos et al. (2003) is lower than the obtained in this study.

For investigating the wavelength dependence of σ_{sca}, we calculated the Angstrom exponent α according to the following formula:

$$\alpha = \frac{-\ln[\sigma_{sca}(700)/\sigma_{sca}(450)]}{\ln(700/450)}.$$

The Angstrom exponent is an intensive parameter that depends on the aerosol size distribution and refractive index but not on the aerosol concentration and which increases with decreasing particle size. For situations where scattering is dominated by particles of $<1\,\mu m$ diameter (fine), the Angstrom exponent has values around 2 but take values close to 0 when scattering is dominated by particles larger than few microns in diameter (coarse) (Seinfeld and Pandis, 1998). Fig. 3a shows the temporal variation of daily average values of Angstrom exponent. The daily average Angstrom exponent values range from 1 to 2, suggesting a larger fraction of submicron particles at the site, an observation confirmed by measurements of aerosol size distribution by APS (Fig. 3b). This last figure shows the temporal evolution of the mean daily values of the ratio N_F/N_C which represents the relative abundance of "fine"

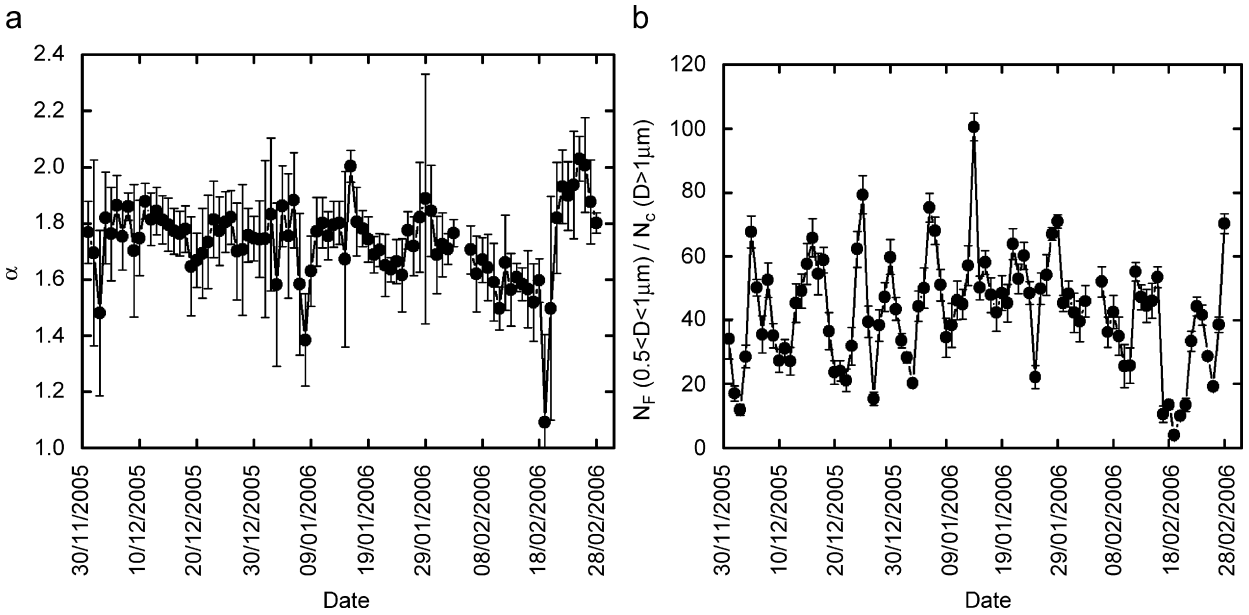

Fig. 3. Daily mean values and standard deviations of (a) the Angstrom exponent and (b) N_F/N_C for winter 2005–2006.

aerosols N_F ($0.5<D<1\,\mu m$) and coarse N_C ($1<D<20\,\mu m$). As it is clear from Fig. 3b, there was a large predominance of "fine" particles ($0.5<D<1\,\mu m$) at the study site.

Based on the measurements of σ_{sca} and σ_{abs} and considering the Angstrom exponent we calculated the single scattering albedo at 670 nm, ω_{0A} (670 nm), which is the ratio between σ_{sca} and $\sigma_{sca}+\sigma_{abs}$. Purely scattering aerosols (e.g. sulfate) exhibit values of $\omega_{0A}=1$, while very strong absorbers (e.g. black carbon) have values of 0.3. In Fig. 4, we present the temporal evolution of daily average values of single scattering albedo at 670 nm. The daily averages single scattering albedo ranged from 0.5 to 0.8 with mean value of 0.66 ± 0.06, indicating that about 35% of the aerosol light extinction was due to absorption. The single scattering albedo values obtained in Granada are similar to the mean value of 0.68 ± 0.07 obtained at the Pedregal site, Mexico City, by Eidels-Dubovoi (2002) and are in the range (0.5–0.85) reported for urban sites in US (Waggoner et al., 1981). Nevertheless, the single scattering albedo measured in Granada is lower than those obtained in Atlanta (0.87 ± 0.08) and Beijing, China (0.81 ± 0.08) by Carrico et al. (2003) and Bergin et al. (2001), respectively. The lower values of single scattering albedo in urban areas are generally related to black carbon formation from combustion sources, although dust can also contribute to aerosol light absorption (Horvath, 1998; Bobren and Huffman, 1983). Thus, the lower scattering albedo at Granada reflects the greater relative importance of light absorbing aerosols and indicates that the Granada aerosols contain a large fraction of absorbing material.

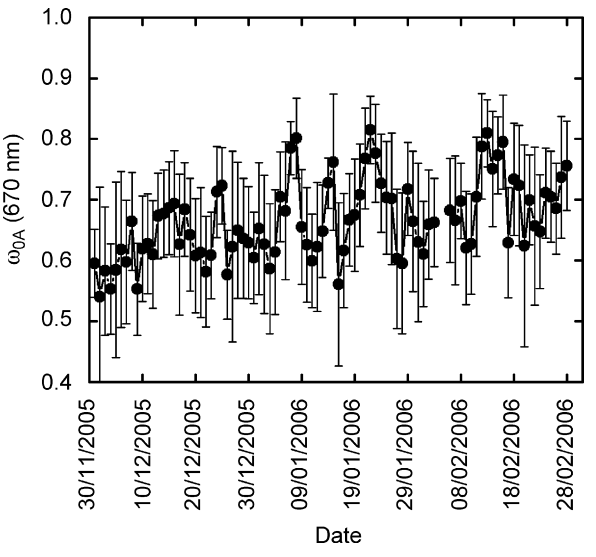

Fig. 4. Daily mean values and standard deviation ω_{0A} (670 nm) for winter 2005–2006.

We calculated the ratio σ_{bsca} (550 nm)/σ_{sca} (550 nm) called backscatter ratio, β_{sca}. This parameter is commonly required in radiative transfer models for the estimation of aerosol-scattered radiation reaching the ground (Iqbal, 1983). The daily averages backscatter ratio at 550 nm ranged from 0.10 to 0.16 with mean value of 0.13 ± 0.01 that is similar to the mean backscatter ratio of $0.13\pm0.02\,M\,m^{-1}$ obtained by Andreae et al. (2002) in Sde Boker (Israel), under continental pollution conditions.

4.2. Diurnal variations of aerosol properties

To investigate the diurnal variability of the aerosol properties, we used 5-min averages of directly and indirectly measured quantities. Fig. 5 shows values of σ_{sca} (550 nm), σ_{abs} (670 nm), α, N_F/N_C, N_F, N_C and ω_{0A} (670 nm) averaged for each hour of the day as function of time, with the error bars representing ±1 S.D. There were clear diurnal patterns in all these aerosol properties. As is clear from Fig. 5a, the diurnal patterns of σ_{sca} and σ_{abs} were similar, with high values in the morning period (08:00–11:00 GMT) which decreased and reached minimum in the afternoon period (around 15:00–16:00 GMT). During the late afternoon σ_{sca} and σ_{abs} again showed increasing trends and reached peak values around 19:00–21:00 GMT. These diurnal cycles are typical of urban areas (Horvath et al., 1997) and are likely due to variations in emission sources and meteorological conditions. The mean daily pattern of ambient temperature, wind speeds and relative humidity for the analyzed period are given in Fig. 6.

The high values of σ_{sca} and σ_{abs} during the early morning could be attributed to elevated emissions associated with the traffic during the morning rush hour as well as low wind speeds and also low ambient temperature (Fig. 6) and hence low mixing height resulting in high aerosol concentrations at surface. The morning peak is particularly pronounced for σ_{abs} that showed substantial increases by factor of 3.6 from about 15 to $55\,M\,m^{-1}$, while σ_{sca} increased by factor of 2.2 from about 65 to $146\,M\,m^{-1}$. This could be explained by the large black carbon fraction contained in the fresh

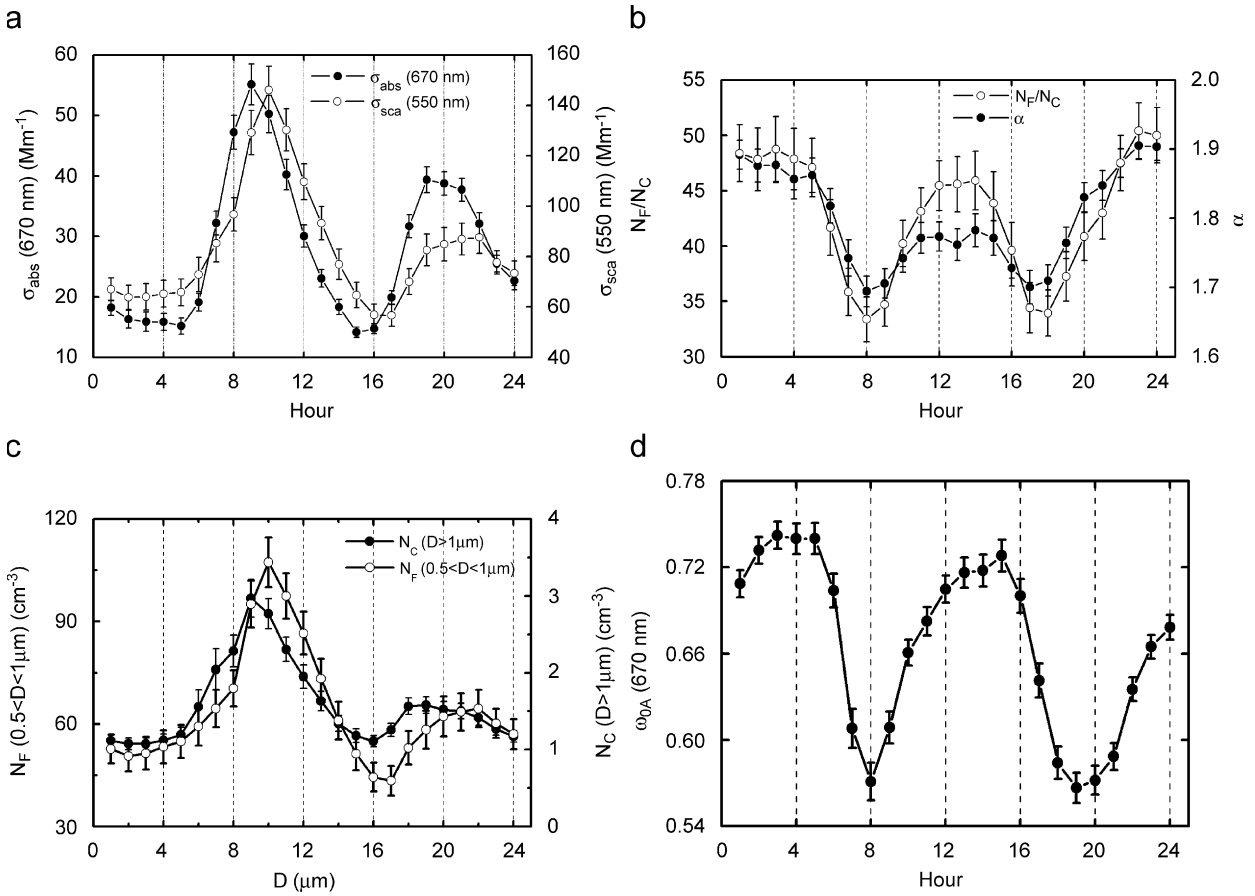

Fig. 5. Diurnal variation of hourly averaged (a) σ_{sca} (550 nm) and σ_{abs} (670 nm), (b) N_F/N_C and α, (c) N_F ($0.5<D<1\,\mu m$) and N_C ($D>1\,\mu m$) and (d) ω_{0A} (670 nm) for winter 2005–2006 at Granada. The vertical error bars represent ± 1 S.D.

combustion aerosols from diesel vehicles. It is interesting to note that the σ_{abs} reached its maximum value (at 09:00 h) before the σ_{sca}, which reached its maximum 1 h later. The later scattering peak could be attributed to secondary aerosols formed photo-chemically in the atmosphere while the early absorption peak could be attributed to primary aerosols (black carbon) traffic emissions during the morning rush hour traffic. The following steady decrease in σ_{sca} and σ_{abs} could be associated with the increase in ambient temperature (Fig. 6) and thus in the vertical convective activity permitting an increased vertical dispersion of aerosol, and also with the increase in the wind speeds and decrease in the vehicle density. The daily σ_{sca} and σ_{abs} minimum values occurred at around 15:00–16:00 h and were associated with maxima in temperature and wind speeds and with minima in relative humidity (Fig. 6) and traffic density. The increase in σ_{sca} and σ_{abs} during late evening could be caused by the evening traffic peak which begins at 17:00 GMT as well as decreasing mixing height and wind speeds. However, the scattering and absorption coefficients in the late evening were lower than those in the morning. This was because of the lower ambient temperature (Fig. 6) and hence lower mixing height in the morning period than in the late afternoon. Also, the wind speeds were relatively lower in the morning period than in the afternoon (Fig. 6).

The diurnal cycles of hourly average α and N_F/N_C were similar, with high values during night and minimum values in the morning and the afternoon traffic rush hours (Fig. 5b). The large values of α (>1.7) and N_F/N_C (>35) show a larger fraction of submicron particles at the site. Also, N_F and N_C show a similar pattern with high values during morning and afternoon traffic rush hours (Fig. 5c). During the traffic rush hours, the vehicles emit fresh pollutants which are not only smaller in size but also

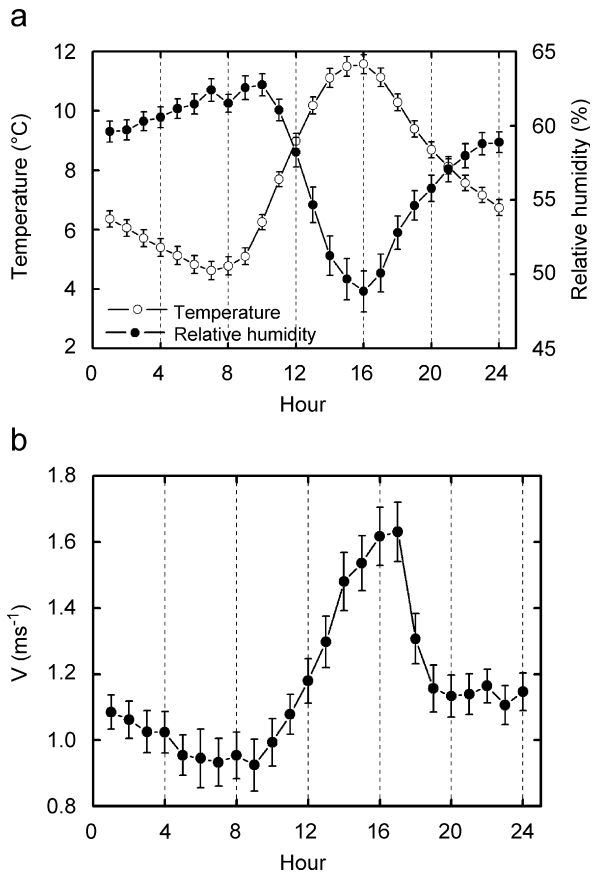

Fig. 6. Diurnal variation of hourly averaged (a) temperature and relative humidity and (b) wind velocity for winter 2005–2006 at Granada. The vertical error bars represent ± 1 S.D.

enhance the dispersion of road dust (large particles) into the air. This could explain the increased fraction of micrometric particles (high values of N_C) during morning and afternoon traffic rush hours. Also, it is interesting to note that N_C reaches its maximum value before N_F (Fig. 5c). This time delay of the N_F peak could be attributed to the secondary origin of the associated aerosol particles. On the other hand, the temporal pattern of N_C reflects that this range of aerosol particles correspond to primary particles associated to road dust dispersed by vehicles into the air during traffic rush hours. The diurnal single scattering albedo pattern also showed similar behavior with minimum values during morning and late afternoon traffic rush hours (Fig. 5d). The lower values of ω_{0A} (670 nm) demonstrate a greater relative importance of light absorbing particles during traffic rush hours and the importance of traffic emissions.

4.3. Weekly variation of aerosol properties

Traffic is one of the most important sources of aerosol pollution in urban areas. The traffic density in Granada, like in other urban regions of the world, varies substantially between weekdays and weekend, with a strong decrease on the weekend due to holidays for offices, schools and other urban activities. On the other hand, domestic heating emissions are also an active source of aerosol in Granada during winter but are not expected to show large variation during the week. Thus, the comparison of aerosol properties corresponding to weekdays and weekend can be used to show the influence of traffic source on the aerosol properties and to investigate the contribution of traffic emissions to the urban aerosol in Granada.

To determine the weekly aerosol characteristics, all aerosol properties analyzed here were averaged for each day of the week using 1-h mean data from the entire study period. Weekly patterns of hourly average aerosol data grouped by day of the week are shown in Fig. 7. As can be seen, weekly variation suggests that the average aerosol absorption coefficient gradually increased from Monday to Thursday and then decreased from Friday to Sunday. The σ_{abs} has high values from Wednesday to Friday and reached its maximum value of about 33.5 M m^{-1} on Thursday. The σ_{abs} values were low on Saturday and Sunday with minimum value of about 21.0 M m^{-1} occurring on Sunday, suggesting $>35\%$ reduction in σ_{abs} during the weekend compared to the mid-week (Wednesday–Friday) high values of σ_{abs}. The considerable reduction in σ_{abs} during weekend period could be related to the reduction in the traffic density and human activities and thus to the reduction in pollutant emissions.

On other hand, the σ_{sca} showed a distinct weekly variation with minimum values occurring on Tuesday. Opposite to σ_{abs}, the σ_{sca} did not show its lowest values during the weekend, and the aerosol scattering coefficient obtained during Saturday and Sunday was higher than that obtained for Monday and Tuesday. The large weekend values of σ_{sca} could be indicative of aged aerosols. The increase in precursor-gas emissions (due to traffic) during weekdays enhances formation of new secondary aerosols. Subsequent growth of these secondary aerosols would lead to increased concentrations of accumulation-mode aerosol and hence to high values of σ_{sca} on weekend days. The permanence

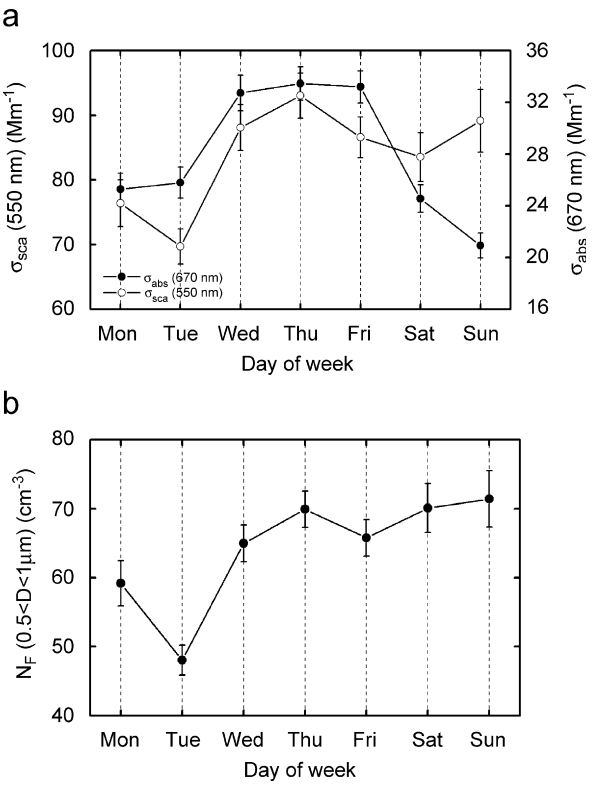

Fig. 7. Day of week variation in (a) σ_{sca} (550 nm) and σ_{abs} (670 nm) and (b) concentration of particles with $D<1\,\mu m$ for winter 2005–2006 at Granada. The vertical error bars represent ± 1 S.D.

of the aerosol near the sources is a result of the topography of the area and the typical prevalence of high-pressure systems during winter. In this sense, the reduced wind speeds do not allow an appropriate horizontal dispersion of the emitted pollutants. These results are corroborated by the analysis of aerosol concentrations in the 0.5–1 μm diameter range obtained by aerodynamic aerosol sizer (APS-3321; TSI) that shows a weekly average pattern with large concentrations on weekend and low values on Tuesday (Fig. 7). Particles in this diameter range are mainly from secondary origins and are in the size range that significantly affects nephelometer scattering measurements. The lowest σ_{sca} values observed on Monday and Tuesday could be related to the reduction in the emissions of precursor gases during weekend due to the reduction in the traffic density which leads to the reduction in the concentration of secondary aerosol in accumulation mode during the two first days of the week (Fig. 7) and low values of σ_{sca}.

5. Conclusion

The average values of the aerosol scattering coefficient at 550 nm, σ_{sca}, and the aerosol absorption coefficient at 670 nm, σ_{abs}, measured in Granada (Spain) during winter 2005–2006 are $80 \pm 60\,M\,m^{-1}$ ($\pm$S.D.) and $30 \pm 20\,M\,m^{-1}$, respectively. The Angstrom exponent presented an average value of 1.8 ± 0.3, suggesting a large fraction of fine particles at the site, an observation confirmed by aerosol size distribution measurements. Urban aerosols in Granada contain a large fraction of absorbing material as indicated by an average single-scattering albedo throughout the studied period of 0.66, indicating that about 35% of the aerosol light extinction was accounted for by absorption. There was significant amount of day-to-day variability in aerosol scattering and absorption coefficients as well as aerosol concentrations. The lowest σ_{sca} and σ_{abs} values were recorded on the same day and were associated with a rain event and relatively high wind speeds. Backward trajectory analysis was used to characterize the origin and the transport pathways of air masses reaching our study area and to identify the sources regions causing high aerosol loadings. The highest σ_{sca} value was related to the influence of air masses that passed over polluted areas in Europe and also to local stagnation conditions, while the highest σ_{abs} value was linked to dust transport from North Africa. A clear diurnal pattern was observed in scattering and absorption coefficients and particle concentrations with two local maxima occurring in early morning and late evening. This diurnal cycle is typical of urban areas and was likely due to variations in emission sources and meteorological conditions. Significant reduction in σ_{abs} values has been found on weekends compared to weekdays indicating a strong impact of traffic emissions on absorbing aerosol concentrations. In contrast to σ_{abs}, the aerosol scattering coefficient obtained during weekends was higher than that obtained on Monday and Tuesday. High weekend values of σ_{sca} have been related to aged aerosols.

Acknowledgments

This work was supported by CICYT from the Spanish Ministry of Science and Technology through projects Nos. CGL2004-05984-C07-03 and REN2003-03175. The authors would like to express their gratitude to the NASA/Goddard

Space Flight Center, NOAA Air Resources Laboratory (ARL) for the provision of the HYSPLIT transport and dispersion model. We thank Dr. Kowalski who revised the English translation of the manuscript.

References

Adam, M., Pahlow, M., Kovalev, V.A., Ondov, J.M., Parlange, MB., Nair, N., 2004. Aerosol optical characterization by nephelometer and lidar: the Baltimore Supersite experiment during the Canadian forest fire smoke intrusion. Journal of Geophysical Research 109 doi:10.1029/2003JD004047, NO.D16S02.

Alados-Arboledas, L., Lyamani, H., Olmo, F.J., 2003. Aerosol size properties at Armilla, Granada (Spain). Quarterly Journal of the Royal Meteorological Society 129 (590), 1395–1413.

Anderson, T.L., Covert, D.S., Marshall, S.F., Laucks, M.L., Charlson, R.J., Waggoner, A.P., Ogren, J.A., Caldow, R., Holm, R.L., Quant, F.R., Sem, G.J., Wiedensohler, A., Ahlquist, N.C., Bates, T.S., 1996. Performance characteristics of high sensitivity, three-wavelength, total scatter/backscatter nephelometer. Journal of Atmospheric and Oceanic Technology 13, 967–986.

Anderson, T.L., Ogren, J.A., 1998. Determining aerosol radiative properties using the TSI 3563 integrating nephelometer. Aerosol Science and Technology 29, 57–69.

Andreae, T.W., Andreae, M.O., Ichoku, C., 2002. Light scattering by dust and anthropogenic aerosol at a remote site in the Negev Desert, Israel. Journal of Geophysical Research 107 doi:10.1029/2001JD900252, NO.D2.

Baron, P.A., Willeke, K., 2001. Aerosol Measurement. Principles, Techniques, and Applications. Wiley.

Bergin, M.H., Cass, G., Xu, J., Fang, C., Zeng, L., Yu, T., Kiang, C.S., Chameides, W.L., 2001. Aerosol radiative, physical and chemical properties in Beijing during June 1999. Journal of Geophysical Research 106, 17969–17980.

Bobren, F., Huffman, D.R., 1983. Absorption and scattering by small particles. Wiley, New York, pp. 530.

Carrico, C.M., Bergin, M.H., Xu, J., 2003. Urban aerosol radiative properties: measurements the during 1999 Atlanta Supersite Experiment. Journal of Geophysical Research 108 doi:10.1029/2001JD001222, NO.D7, 8422.

D'Almeida, G.A., Keopke, P., Shettle, E.P., 1991. In: Deepak, A. (Ed.), Atmospheric Aerosol: Global Climatology and Radiative Characteristics. A. Deepak Publishing, Hampton, VA.

Dockery, D., Pope, A., 1996. Epidemiology of acute health effects: summary of time-series. In: Wilson, R., Spengler, J.D. (Eds.), Particles in Our Air: Concentration and Health Effects. Harvard University Press, Cambridge, MA, pp. 123–147.

Draxler, R.R., Rolph, G.D., 2003. HYSPLIT (HYbrid Single-Particle Lagrangian Integrated Trajectory) Model access via NOAA ARL READY Website 〈http://www.arl.noaa.gov/ready/hysplit4.html〉, NOAA Air Resources Lab., Silver Spring, MD.

Eidels-Dubovoi, S., 2002. Aerosol impacts on visible light extinction in the atmosphere of Mexico City. The Science of the Total Environment 287, 213–220.

Gerasopoulos, E., Andreae, M.O., Zeferos, C.S., Andreae, T.W., Balis, D., Formenti, P., Merlet, P., Amiridis, V., Papastefanou, C., 2003. Climatological aspects of aerosol optical properties in Northern Greece. Atmospheric Chemistry and Physics Discussions 3, 2059–2099.

Haywood, J.M., Shine, K.P., 1995. The effect of anthropogenic sulphate and soot aerosol on the clear sky planetary radiation budget. Geophysical Research Letter 22, 603–606.

Haywood, J.M., Shine, K.P., 1997. Multi-spectral calculations of the direct radiative forcing of tropospheric sulphate and soot aerosols using a column model. Quarterly Journal of the Royal Meteorological Society—Part A 123 (543), 1907–1930.

Hitzenberger, R., Tohno, S., 2001. Comparison of black carbon (BC) aerosols in two urban areas-concentration and size distributions. Atmospheric Environment 35, 2153–2167.

Horvath, H., 1995. Estimation of the average visibility in central Europe. Atmospheric Environment 29, 241–246.

Horvath, H., 1996. Spectral extinction coefficients of rural aerosol in southern Italy—a case study of cause and effect of variability of atmospheric aerosol. Journal of Aerosol Science 27 (3), 437–453.

Horvath, H., 1998. In: Harrison, R.M., van Grieken, R. (Eds.), Influence of atmospheric aerosols upon the global radiation balance, in atmospheric particles. Wiley, Hoboken, NJ, pp. 543–596.

Horvath, H., Catalan, L., Trier, A., 1997. A study of aerosol of Santiago de Chile III: light absorption measurements. Atmospheric Environment 31, 3737–3744.

Iqbal, M., 1983. Introduction to Solar Radiation. Academic Press, Canada, Ont.

Kaufman, Y.J., Koren, I., Remer, L.A., Rosenfeld, D., Rudich, Y., 2005. The effect of smoke, dust, and pollution aerosol on shallow cloud development over the Atlantic Ocean. Proceedings of the National Academy of Sciences of the United States of America 102 (32), 11207–11212.

Lyamani, H., Olmo, F.J., Alados-Arboledas, L., 2005. Saharan dust outbreak over south-eastern Spain as detected by sun photometer. Atmospheric Environment 39, 7276–7284.

Lyamani, H., Olmo, F.J., Alcantara, A., Alados-Arboledas, L., 2006a. Atmospheric aerosols during the 2003 heat wave in southeastern Spain I: spectral optical depth. Atmospheric Environment 40, 6453–6464.

Lyamani, H., Olmo, F.J., Alcantara, A., Alados-Arboledas, L., 2006b. Atmospheric aerosols during the 2003 heat wave in southeastern Spain II: microphysical columnar properties and radiative forcing. Atmospheric Environment 40, 6465–6476.

Park, S.S., Kim, Y.J., Fung, K., 2002. $PM_{2.5}$ carbon measurements in two urban areas: Seoul and Kwangju, Korea. Atmospheric Environment 36, 1287–1297.

Petzold, A., Schönlinner, M., 2004. Multi-angle Absorption photometry—a new method for the measurement of aerosol light absorption and atmospheric black carbon. Journal of Aerosol Science 35, 421–441.

Petzold, A., Schloesser, H., Sheridan, P.J., Arnott, W.P., 2005. Evaluation of multi-angle absorption photometry for measuring aerosol light absorption. Aerosol Science and Technology 39, 40–51.

Rodríguez, S., Querol, X., Alastuey, A., Kallos, G., Kakaliagou, O., 2001. Saharan dust contribution to PM10 and TSP levels

in Southern and Eastern Spain. Atmospheric Environment 35, 2433–2447.

Saha, A., Despiau, S., 2006. Seasonal and diurnal variations of black carbon aerosols over an urban–costal zone. In: Proceedings of Conference on Visibility, Aerosol, and Atmospheric Optic (2006).

Seinfeld, J.H., Pandis, S.N., 1998. Atmospheric Chemistry and Physics: From Air Pollution to Climate Change. Wiley, New York, 1326pp.

Targino, A.C., Noone, K.J., Öström, E., 2005. Airborne in situ characterization of dry aerosol optical properties in multi-source influenced marine region. Tellus 57B (3), 247–260.

ten Brink, H.M., Veefkind, J.P., Waijers-Ijpelaan, A., van der Hge, J.C., 1996. Aerosol light scattering in the Netherlands. Atmospheric Environment 30, 4251–4261.

Volcken, J., Peters, T.M., 2003. Counting and particle transmission efficiency of the aerodynamic particle sizer. Aerosol Science 36, 1400–1408.

Waggoner, A.P., Weiss, R.E., Ahlquist, N.C., Covert, D.S., Will, S., Charlson, R.J., 1981. Optical characteristics of atmospheric aerosols. Atmospheric Environment 15, 1891–1909.

Xu, J., Bergin, M.H., Yu, X., Liu, G., Zhao, J., Carrico, C.M., Baumann, K., 2002. Measurement of aerosol chemical, physical and radiative properties in the Yangtze delta region of China. Atmospheric Environment 36, 161–173.